

Quenched lattice calculation of semileptonic heavy-light meson form factors

G.M. de Divitiis^{a,b}, R. Petronzio^{a,b}, N. Tantalo^{b,c}

^a *Università di Roma “Tor Vergata”, I-00133 Rome, Italy*

^b *INFN sezione di Roma “Tor Vergata”, I-00133 Rome, Italy*

^c *Centro Enrico Fermi, I-00184 Rome, Italy*

We calculate, in the continuum limit of quenched lattice QCD, the matrix elements of the heavy-heavy vector current between heavy-light pseudoscalar meson states. We present the form factors for different values of the initial and final meson masses at finite momentum transfer. In particular we study the dependence upon the heavy quark masses and extract the Isgur-Wise function.

I. INTRODUCTION

Semileptonic decays of heavy-light mesons play a central role in the study of flavour physics both on the experimental and theoretical sides. The extraction of the Cabibbo–Kobayashi–Maskawa [1, 2] matrix element V_{cb} , for example, requires the experimental measurement of the decay rate of the process $B \rightarrow D^{(*)} \ell \nu$ and the theoretical calculation of the hadron matrix elements of the flavour changing weak currents. A non-perturbative estimate of the matrix elements can be obtained by lattice QCD. Furthermore, within the heavy quark effective theory (HQET) it has been shown [3] that the semileptonic transitions of a heavy-light meson into another heavy-light meson can be parametrized, at leading order of the expansion in the inverse heavy quark mass, in terms of a universal form factor known as Isgur-Wise function. The Isgur-Wise function is universal in the sense that it describes any semileptonic decay mediated by heavy-heavy weak currents regardless of the flavour of the initial and final heavy quarks and of the spins of the mesons. From the phenomenological point of view it is relevant to know the size of the corrections to the Isgur-Wise limit and to establish at which order the heavy quark expansion has to be truncated to produce useful results down to the charm mass.

In this work we perform a non-perturbative calculation by relying on the quenched approximation. A subset of results with a phenomenological discussion has been already presented in ref. [4]. Here we present detailed results of continuum and chiral extrapolations and separate estimates of the two independent form factors for several values of the initial and final heavy quark masses together with an analysis of the infinite heavy quark mass limit. The simulation of relativistic heavy quarks with masses ranging from the physical b mass down to the physical c mass was performed by using the step scaling method (SSM) [5], already applied successfully to the determination of heavy quark masses and heavy-light meson decay constants [6, 7, 8]. The SSM allows to reconcile large quark masses with adequate lattice resolution and large physical volumes. The two form factors that parametrize the matrix elements have been calculated for different values of the momentum transfer by making use of flavour twisted boundary conditions [9], that shift the discretized set of lattice momenta by an arbitrary amount (see also [10, 11]).

The plan of the paper is as follows. In section II we introduce the form factors in the continuum theory and re-derive the Luke’s theorem [12]. In sections III and IV we set up the lattice notation and describe the calculation. In sections V we discuss the results at finite volumes while in section VI we show our final results. We draw our conclusions in section VII.

II. FORM FACTORS

The semileptonic decay of a pseudoscalar meson into another pseudoscalar meson is mediated by the vector part of the weak $V - A$ current. The corresponding matrix element can be parametrized in terms of two form factors,

$$\langle \mathcal{M}_f | V^\mu | \mathcal{M}_i \rangle = (p_i + p_f)^\mu f_+^{i \rightarrow f} + (p_i - p_f)^\mu f_-^{i \rightarrow f}$$

or, equivalently,

$$\frac{\langle \mathcal{M}_f | V^\mu | \mathcal{M}_i \rangle}{\sqrt{M_i M_f}} = (v_i + v_f)^\mu h_+^{i \rightarrow f} + (v_i - v_f)^\mu h_-^{i \rightarrow f} \quad (1)$$

where $v_{i,f} = p_{i,f}/M_{i,f}$ are the 4-velocities of the mesons. The relations between the $h_{\pm}^{i \rightarrow f}$ and the $f_{\pm}^{i \rightarrow f}$ parametrizations are given by

$$h_{\pm}^{i \rightarrow f} = \frac{(M_i + M_f)f_{\pm}^{i \rightarrow f} + (M_i - M_f)f_{\mp}^{i \rightarrow f}}{2\sqrt{M_i M_f}}$$

$$f_{\pm}^{i \rightarrow f} = \frac{(M_i + M_f)h_{\pm}^{i \rightarrow f} - (M_i - M_f)h_{\mp}^{i \rightarrow f}}{2\sqrt{M_i M_f}}$$

In the rest of this paper we work in the $h_{\pm}^{i \rightarrow f}$ parametrization that, as it will emerge from the discussion below, is more convenient for the study of the dependence of the form factors upon the masses of the initial and final heavy quarks.

The form factors depend upon the masses of the parent and daughter particles and upon $w \equiv v_f \cdot v_i$

$$h_{\pm}^{i \rightarrow f}(w) \equiv h_{\pm}(w, M_i, M_f), \quad 1 \leq w \leq (M_i^2 + M_f^2)/2M_i M_f$$

Time reversal and hermiticity imply that $h_{+}^{i \rightarrow f}$ and $h_{-}^{i \rightarrow f}$ are real. Furthermore they imply that $h_{+}^{i \rightarrow f}$ is even under the interchange of the initial and final states while $h_{-}^{i \rightarrow f}$ is odd,

$$h_{+}(w, M_i, M_f) = h_{+}(w, M_f, M_i), \quad h_{-}(w, M_i, M_f) = -h_{-}(w, M_f, M_i) \quad (2)$$

In eq. (1) one can consider the limit in which one of (or both) meson masses goes to infinity at fixed 4-velocity; the left hand side is well defined in this limits and, consequently, also the form factors. It is thus legitimate to make a change of variables from the meson masses to the parameters ε_{+} and ε_{-} , defined as

$$\varepsilon_{+} = \frac{1}{M_f} + \frac{1}{M_i}, \quad \varepsilon_{-} = \frac{1}{M_f} - \frac{1}{M_i}$$

Expressed as functions of the new variables, $h_{\pm}^{i \rightarrow f} \equiv h_{\pm}(w, \varepsilon_{+}, \varepsilon_{-})$ are well defined at $\varepsilon_{+} = 0$ and $\varepsilon_{-} = 0$ and can be expanded in power series around these points. The symmetry properties of eq. (2) force the odd(even) powers of ε_{-} to vanish into the expansion of $h_{+}^{i \rightarrow f}$ ($h_{-}^{i \rightarrow f}$), i.e.

$$h_{+}(w, \varepsilon_{+}, \varepsilon_{-}) = h_{+}(w, 0, 0) + \varepsilon_{+} \frac{\partial h_{+}(w, 0, 0)}{\partial \varepsilon_{+}} + \frac{\varepsilon_{+}^2}{2} \frac{\partial^2 h_{+}(w, 0, 0)}{\partial \varepsilon_{+}^2} + \frac{\varepsilon_{-}^2}{2} \frac{\partial^2 h_{+}(w, 0, 0)}{\partial \varepsilon_{-}^2} + \dots$$

$$h_{-}(w, \varepsilon_{+}, \varepsilon_{-}) = \varepsilon_{-} \frac{\partial h_{-}(w, 0, 0)}{\partial \varepsilon_{-}} + \frac{\varepsilon_{-} \varepsilon_{+}}{2} \frac{\partial^2 h_{-}(w, 0, 0)}{\partial \varepsilon_{-} \partial \varepsilon_{+}} + \dots \quad (3)$$

In the elastic case, when the initial and final mesons coincide, $h_{\pm}^{i \rightarrow i}$ vanishes and the vector current is conserved. The conservation of the vector current implies that $h_{+}^{i \rightarrow i}(w = 1) = 1$. This condition, inserted in the previous equations, translates into a condition on the derivatives of $h_{+}^{i \rightarrow i}$ with respect to ε_{+}

$$\frac{\partial^n h_{+}(w = 1, 0, 0)}{\partial \varepsilon_{+}^n} = 0$$

We thus expect that, for values of $w \simeq 1$ the corrections proportional to ε_{+} will be rather small while the ones proportional to ε_{-} , not constrained by the vector symmetry, can play a role also at zero recoil. This expectation is confirmed by our numerical results (see section VI).

The discussion above is a re-derivation of the "Luke's theorem" [12]. The theorem, originally derived by using HQET arguments, states that $h_{+}^{i \rightarrow i}$ it is not affected by first order corrections at zero recoil. In our language

$$h_{+}(w = 1, \varepsilon_{+}, \varepsilon_{-}) = 1 + \frac{\varepsilon_{-}^2}{2} \frac{\partial^2 h_{+}(w = 1, 0, 0)}{\partial \varepsilon_{-}^2} + \dots \quad (4)$$

Eqs. (3) confirm the analysis of the subleading corrections to the form factors that has been carried out by the authors of ref. [13] within HQET¹. The additional symmetries of the static theory imply relations among the coefficients appearing in eqs. (3) and the corresponding ones arising in the case of vector-pseudoscalar and vector-vector transitions. In particular, $h_+^{i \rightarrow i}$ is proportional at leading order to the Isgur-Wise function [3],

$$h_+(w, 0, 0) = \xi(w), \quad h_-(w, 0, 0) = 0$$

In ref. [4] we have shown the results concerning the form factor $G^{B \rightarrow D}(w)$ that enters into the semileptonic decay rate of a B meson into a D meson in the approximation of massless leptons. This form factor is related to $h_+^{i \rightarrow f}(w)$ and $h_-^{i \rightarrow f}(w)$ by

$$G^{i \rightarrow f}(w) = h_+^{i \rightarrow f}(w) - \frac{M_f - M_i}{M_f + M_i} h_-^{i \rightarrow f}(w)$$

III. LATTICE OBSERVABLES

We have carried out the calculation within the $O(a)$ improved Schrödinger Functional formalism [14, 15] with $T = 2L$ and vanishing background fields. Physical units have been set by using the Sommer's scale and fixing $r_0 = 0.5$ fm [16, 17, 18]. In order to set the notations, we introduce the following source operators

$$O_{sr} = \frac{a^6}{L^3} \sum_{\mathbf{y}, \mathbf{z}} \bar{\zeta}_s(\mathbf{y}) \gamma_5 \zeta_r(\mathbf{z}), \quad O'_{sr} = \frac{a^6}{L^3} \sum_{\mathbf{y}, \mathbf{z}} \bar{\zeta}'_s(\mathbf{y}) \gamma_5 \zeta'_r(\mathbf{z})$$

where s and r are flavour indexes while ζ and ζ' are boundary fields at $x_0 = 0$ and $x_0 = T$ respectively. The bulk operators are defined according to

$$\begin{aligned} A_{sr}^0(x) &= \bar{\psi}_s(x) \gamma_5 \gamma^0 \psi_r(x), & P_{sr}(x) &= \bar{\psi}_s(x) \gamma_5 \psi_r(x) & \mathcal{A}_{sr}^0(x) &= A_{sr}^0(x) + ac_A \frac{\partial_0 + \partial_0^*}{2} P_{sr}(x) \\ V_{sr}^\mu(x) &= \bar{\psi}_s(x) \gamma^\mu \psi_r(x), & T_{sr}^{\mu\nu}(x) &= \bar{\psi}_s(x) \gamma^\mu \gamma^\nu \psi_r(x) & \mathcal{V}_{sr}^\mu(x) &= V_{sr}^\mu(x) + ac_V \frac{\partial_\nu + \partial_\nu^*}{2} T_{sr}^{\mu\nu}(x) \end{aligned}$$

The improvement coefficient c_A has been computed non-perturbatively in ref. [19]. Regarding c_V , we have used the perturbative result from ref. [20] but its actual value influences our results at the level of a few per mille.

The quark masses have been defined through the PCAC relation. We have calculated the following correlation functions

$$f_{sr}^A(x_0) = - \sum_{\mathbf{x}} \langle O_{rs} A_{sr}^0(x) \rangle \quad f_{sr}^P(x_0) = - \sum_{\mathbf{x}} \langle O_{rs} P_{sr}(x) \rangle$$

and defined

$$m_r^{AWI} = \frac{1}{2f_{rr}^P} \left[\frac{\partial_0 + \partial_0^*}{2} f_{rr}^A + ac_A \partial_0 \partial_0^* f_{rr}^P \right], \quad am_r^{VWI} = \frac{1}{2} \left[\frac{1}{k_r} - \frac{1}{k_c} \right]$$

where a is the lattice spacing, k_r is the hopping parameter of the r quark and k_c is the critical value of the hopping parameter. The renormalization group invariant (RGI) quark masses have been obtained by the following relation

$$m_r = Z_M [1 + (b_A - b_P) am_r^{VWI}] m_r^{AWI} \quad (5)$$

The combination $b_A - b_P$ of the improvement coefficients of the axial current and pseudoscalar density has been computed non-perturbatively in [21, 23]. The factor Z_M is known with very high precision in a range of inverse bare

¹ Some care is needed when eqs. (3) are compared with the corresponding results of ref. [13]. Indeed eqs. (3) are the result of a Taylor expansion and the coefficients do not depend upon $\varepsilon_{+,-}$ and, consequently, upon the meson masses. Eqs. (B1) of ref. [13] are expansions in inverse powers of the quark masses that depend upon the renormalization scale as well as the coefficients. This dependence cancels at any given order.

couplings that does not cover all the values of β used in our simulations. We have used the results reported in table 6 of ref. [22] to parametrize Z_M in the enlarged range of β values [5.9, 7.6].

In order to define on the lattice the matrix elements of the vector current between pseudoscalar meson states, we need to introduce other two correlation functions,

$$\mathcal{F}_{i \rightarrow f}^\mu(x_0; \mathbf{p}_i, \mathbf{p}_f) = \frac{a^3}{2} \sum_{\mathbf{x}} \langle O_{li} \mathcal{V}_{if}^\mu(x) O'_{fl} \rangle, \quad f_{\mathcal{A}}^f(x_0, \mathbf{p}_f) = - \sum_{\mathbf{x}} \langle O_{lf} \mathcal{A}_{fl}^0(x) \rangle$$

where i and f are the heavy flavour indexes and l is the light one. The external momenta have been set by using flavour twisted b.c. for the heavy flavours; in particular we have used

$$\psi_{i,f}(x + \hat{1}L) = e^{i\theta_{i,f}} \psi_{i,f}(x), \quad p_1 = \frac{\theta_{i,f}}{L} + \frac{2\pi k_1}{L}, \quad k_1 \in \mathbb{N}$$

and ordinary periodic b.c. in the other spatial directions and for the light quarks. We have worked in the Lorentz frame in which the parent particle is at rest ($\mathbf{p}_i = \mathbf{0}$). In this frame w is simply expressed in terms of the ratio between the energy and the mass of the daughter particle $w = E_f/M_f$. The matrix elements of V^μ have been defined by the following ratios

$$\langle V^\mu \rangle_{D1}^{i \rightarrow f} \equiv \langle \mathcal{M}_f | V^\mu | \mathcal{M}_i \rangle_{D1} \equiv 2\sqrt{M_i E_f} \frac{\mathcal{F}_{i \rightarrow f}^\mu(T/2; \mathbf{0}, \mathbf{p}_f)}{\sqrt{\mathcal{F}_{i \rightarrow i}^0(T/2; \mathbf{0}, \mathbf{0}) \mathcal{F}_{f \rightarrow f}^0(T/2; \mathbf{p}_f, \mathbf{p}_f)}} \quad (6)$$

that become the physical matrix elements in large volumes where single state dominance is a good approximation. An alternative definition of the matrix elements ($D2$), which reduces to the previous one ($D1$) in the infinite volume and at zero lattice spacing, can be obtained by considering

$$\langle V^\mu \rangle_{D2}^{i \rightarrow f} \equiv \langle \mathcal{M}_f | V^\mu | \mathcal{M}_i \rangle_{D2} \equiv 2 \frac{\sqrt{M_i} E_f f_{\mathcal{A}}^f(T/2, \mathbf{0})}{\sqrt{M_f} f_{\mathcal{A}}^f(T/2, \mathbf{p}_f)} \frac{\mathcal{F}_{i \rightarrow f}^\mu(T/2; \mathbf{0}, \mathbf{p}_f)}{\sqrt{\mathcal{F}_{i \rightarrow i}^0(T/2; \mathbf{0}, \mathbf{0}) \mathcal{F}_{f \rightarrow f}^0(T/2; \mathbf{0}, \mathbf{0})}} \quad (7)$$

In eqs. (6) and (7) the renormalization factors Z_V and Z_A cancel in the ratios together with the factors containing the improvement coefficients b_V and b_A .

By calculating the following ratio

$$x_f = \frac{\mathcal{F}_{f \rightarrow f}^1(T/2; \mathbf{0}, \mathbf{p}_f)}{\mathcal{F}_{f \rightarrow f}^0(T/2; \mathbf{0}, \mathbf{p}_f)} = \frac{\langle \mathcal{M}_f | \mathcal{V}^1 | \mathcal{M}_f \rangle}{\langle \mathcal{M}_f | \mathcal{V}^0 | \mathcal{M}_f \rangle} = \frac{\sqrt{w^2 - 1}}{w + 1}$$

we have defined w , as well as meson masses and energies, entirely in terms of three point correlation functions. This definition of w is noisier than the one that can be obtained in terms of ratios of two point correlation functions; however it leads to exact vector current conservation when $M_f = M_i$ and reduces the final statistical error on the form factors. The two definitions of the matrix elements lead to two definitions of the form factors that, in terms of $\langle V^0 \rangle_D$ and $\langle V^1 \rangle_D$, are expressed by

$$h_+^{i \rightarrow f}(w) = \frac{\langle V^0 \rangle^{i \rightarrow f}}{2M_i \sqrt{r}} \left\{ 1 + \frac{\sqrt{w^2 - 1}}{w + 1} \frac{\langle V^1 \rangle^{i \rightarrow f}}{\langle V^0 \rangle^{i \rightarrow f}} \right\} \quad (8)$$

$$h_-^{i \rightarrow f}(w) = \frac{\langle V^0 \rangle^{i \rightarrow f}}{2M_i \sqrt{r}} \left\{ 1 + \frac{w + 1}{\sqrt{w^2 - 1}} \frac{\langle V^1 \rangle^{i \rightarrow f}}{\langle V^0 \rangle^{i \rightarrow f}} \right\} \quad (9)$$

$$G^{i \rightarrow f}(w) = \frac{2r}{1+r} \frac{\langle V^0 \rangle^{i \rightarrow f}}{2M_i \sqrt{r}} \left\{ 1 + \frac{wr - 1}{r\sqrt{w^2 - 1}} \frac{\langle V^1 \rangle^{i \rightarrow f}}{\langle V^0 \rangle^{i \rightarrow f}} \right\}, \quad r = \frac{M_f}{M_i} \quad (10)$$

The last two equations are not defined at $w = 1$; this is due to the second term in the parenthesis of eq. (9) and (10) that we extrapolate at zero recoil before calculating $h_-^{i \rightarrow f}(w = 1)$ and $G^{i \rightarrow f}(w = 1)$.

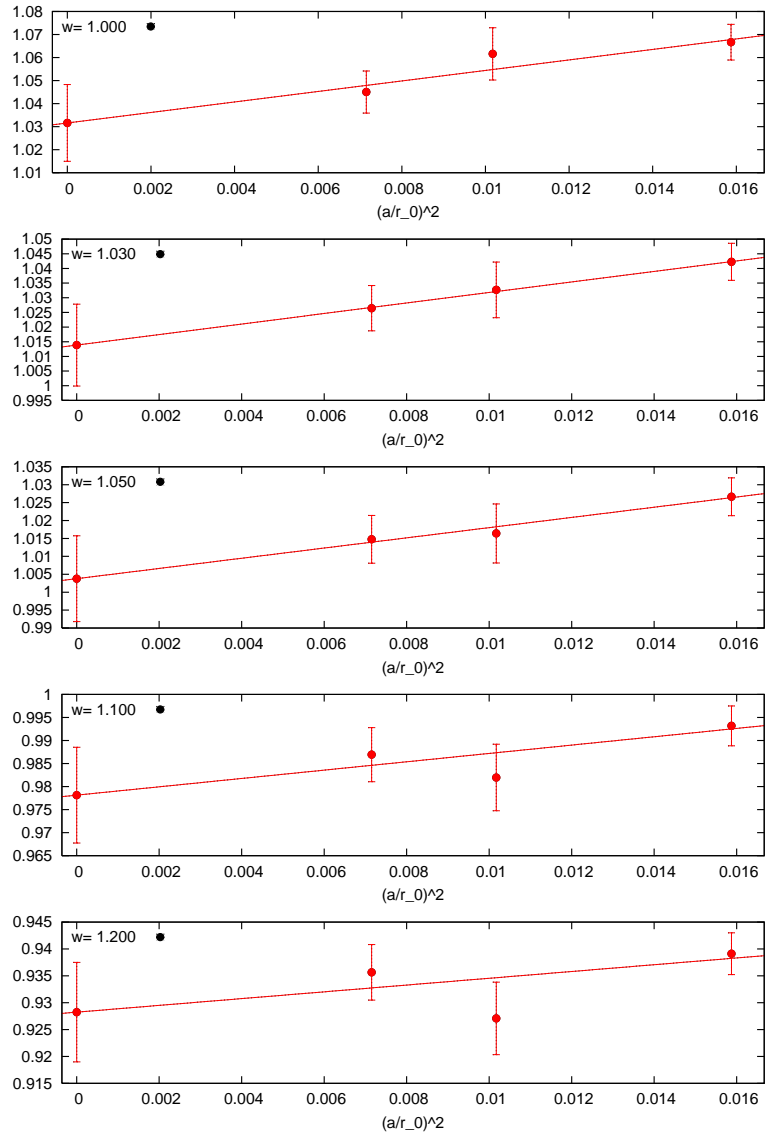


FIG. 1: Extrapolations to the continuum limit of $G^{B \rightarrow D}(w)$. The data correspond to $m_l = m_s$ and to the definition $D1$.

IV. THE STEP SCALING METHOD

The SSM has been introduced to cope with two-scale problems in lattice QCD. In the calculation of heavy-light meson properties the two scales are the mass of the heavy quarks (b, c) and the mass of the light quarks (u, d, s). Here we consider the generic form factor $F^{i \rightarrow f} = \{h_+^{i \rightarrow f}, h_-^{i \rightarrow f}, G^{i \rightarrow f}\}$ as a function of w , the volume L^3 and fix the meson states by the corresponding heavy and light RGI quark masses that, being extracted by the lattice version of the PCAC relation, are not affected by finite volume effects (see eq. 5).

The first step of the finite volume recursion consists in calculating the observable $F^{i \rightarrow f}(w; L_0)$ on a small volume, L_0 , which is chosen to accommodate the dynamics of heavy quarks with masses ranging from the physical value of the charm mass up to the mass of the bottom. As in our previous work we fixed $L_0 = 0.4$ fm. We have simulated five different heavy quark masses $m_{i,f} = \{m_h^1, m_h^2, m_h^3, m_h^4, m_h^5\}$, five different momenta $\theta_1 = \{\theta_1^1, \theta_1^2, \theta_1^3, \theta_1^4, \theta_1^5\}$ (see eq. (6)) and three light quark masses $m_l = \{m_l^1, m_l^2, m_l^3\}$.

A first effect of finite volume is taken into account by evolving the results from L_0 to $L_1 = 0.8$ fm through the factor

$$\sigma^{i \rightarrow f}(w; L_0, L_1) = \frac{F^{i \rightarrow f}(w; L_1)}{F^{i \rightarrow f}(w; L_0)}$$

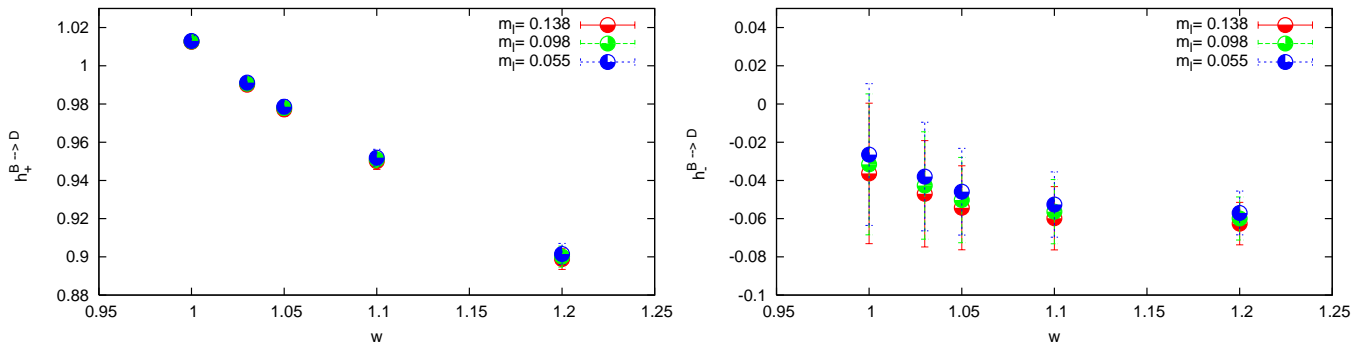


FIG. 2: Light quark mass dependence of $h_+^{B \rightarrow D}(w; L_0)$ (left) and of $h_-^{B \rightarrow D}(w; L_0)$ (right). The different sets of points correspond to different values of m_l ranging from about m_s to about $m_s/4$. The data are in the continuum limit and correspond to the definition D1.

computed for each value of w and for each value of the light quark mass. The crucial point is that the step scaling functions are calculated by simulating heavy quark masses smaller than the b -quark mass. The step scaling functions at $m_i \simeq m_b$ and $m_f \simeq m_c$ are obtained by directly simulating m_f both on L_0 and on L_1 and by a smooth extrapolation in $1/m_i$.

Extrapolating the step scaling functions is more advantageous than extrapolating the form factors. This can be easily understood by relying on HQET expectations (see also eq. (3)),

$$\begin{aligned}
 \sigma^{i \rightarrow f}(w; L_0, L_1) &= \frac{F^{(0) \rightarrow f}(w; L_1) \left[1 + \frac{F^{(1) \rightarrow f}(w; L_1)}{m_i} + \dots \right]}{F^{(0) \rightarrow f}(w; L_0) \left[1 + \frac{F^{(1) \rightarrow f}(w; L_0)}{m_i} + \dots \right]} \\
 &= \frac{F^{(0) \rightarrow f}(w; L_1)}{F^{(0) \rightarrow f}(w; L_0)} \left[1 + \frac{F^{(1) \rightarrow f}(w; L_1) - F^{(1) \rightarrow f}(w; L_0)}{m_i} + \dots \right] \\
 &\equiv \sigma^{(0) \rightarrow f}(w; L_0, L_1) \left[1 + \frac{\sigma^{(1) \rightarrow f}(w; L_0, L_1)}{m_i} + \dots \right]
 \end{aligned}$$

In the previous relations the superscripts in parenthesis, (n), mark the order of the expansion in the inverse heavy quark mass. The subleading correction to the step scaling functions is the difference of two terms and vanishes in the infinite volume, $\sigma^{(1) \rightarrow f}(w; L_0, L_1) = F^{(1) \rightarrow f}(w; L_1) - F^{(1) \rightarrow f}(w; L_0)$, becoming smaller and smaller as the volume is increased. This matches the general idea that finite volume effects, measured by the σ 's, are almost insensitive to the high energy scale.

We also compute the step scaling functions of the elastic form factors $h_+^{i \rightarrow i}$ at $m_i \simeq m_b$ by extrapolating the corresponding results from smaller heavy quark masses. Also in this case the σ 's are expected to be almost flat with respect to $1/m_i$.

In order to remove the residual finite volume effects we iterate the procedure described above once more passing from L_1 to $L_2 = 1.2$ fm. Our final results are obtained from

$$F^{i \rightarrow f}(w; L_2) = F^{i \rightarrow f}(w; L_0) \sigma^{i \rightarrow f}(w; L_0, L_1) \sigma^{i \rightarrow f}(w; L_1, L_2) \quad (11)$$

V. FINITE VOLUME RESULTS

A. small volume

The small volume $L_0 = 0.4$ fm has been simulated by using three different values of the lattice spacing (see table II). The small physical extent of the volume allowed us to simulate relativistic heavy quarks with masses ranging from

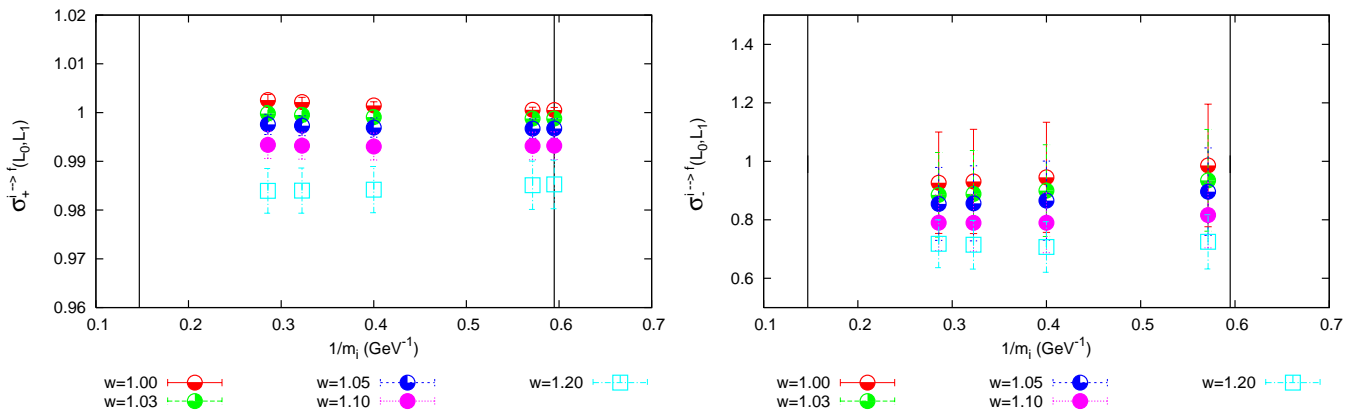


FIG. 3: Step scaling functions of $h_+^{i \rightarrow c}$ (left) and $h_-^{i \rightarrow c}$ (right) as functions of $1/m_i$ for the first evolution step (from L_0 to L_1). The black vertical lines represent the physical points $m_i = m_c$ and $m_i = m_b$. The data are in the continuum and chiral limits and correspond to the definition D1.

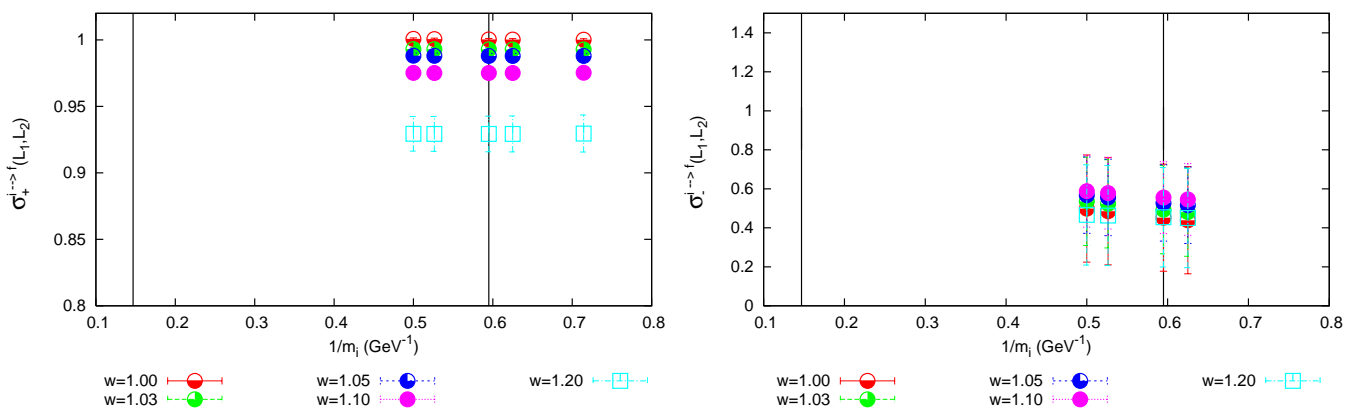


FIG. 4: Step scaling functions of $h_+^{i \rightarrow f}$ (left) and $h_-^{i \rightarrow f}$ (right) at fixed m_f as functions of $1/m_i$ for the second evolution step (from L_1 to L_2). The black vertical lines represent the physical points $m_i = m_c$ and $m_i = m_b$. The data are in the continuum and chiral limits and correspond to the definition D1.

around m_b down to m_c . We have computed the form factors $h_+^{i \rightarrow f}$, $h_-^{i \rightarrow f}$ and $G^{i \rightarrow f}$ for all the combinations of heavy and light quark masses and for five different values of the momentum transferred.

In figure 1 we show the continuum extrapolations of $G^{B \rightarrow D}(w)$. The points in this figure correspond to $m_l = m_s$ but similar figures can be obtained for the other values of the light and heavy quark masses and for the other form factors.

In figure 2 we show $h_+^{B \rightarrow D}$ (left) and $h_-^{B \rightarrow D}$ (right) as functions of w for the three different values of light quark masses that we have simulated (ranging from about m_s to $m_s/4$). As we have anticipated in ref. [4], we find that the F 's behave as constants with respect to m_l within the statistical errors. This happens for each combination of heavy quark masses and for each value of the lattice spacing. Nevertheless we make a linear extrapolation to reach the chiral limit; the resulting error largely accounts for the systematics due to these extrapolations. In the following our results include the mild chiral extrapolation.

B. steps

The parameters of the simulations of the first evolution step (from L_0 to L_1) are shown in table IV. The maximum value of the heavy quark mass has been reduced to $m_h \simeq m_b/2$. In figure 3 we can test our hypothesis on the low sensitivity of the step scaling functions upon the high energy scale. The figure shows the step scaling functions of the form factors $h_+^{i \rightarrow c}$ (left) and $h_-^{i \rightarrow c}$ (right) as functions of $1/m_i$. In both cases the dependence upon m_i is hardly

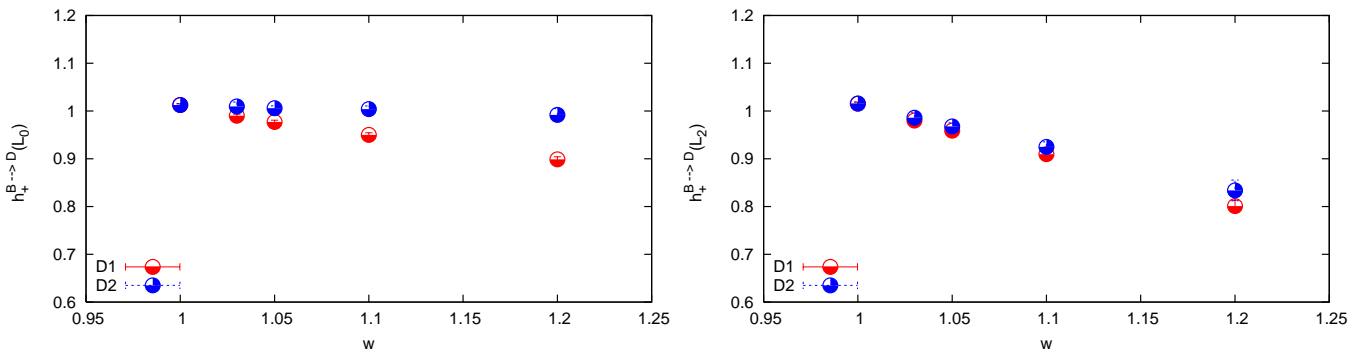


FIG. 5: Comparison of the two definitions of $h_+^{B \rightarrow D}(w; L)$ at $L_0 = 0.4$ fm (left) and at $L_2 = 1.2$ fm (right). The data are in the continuum and chiral limits.

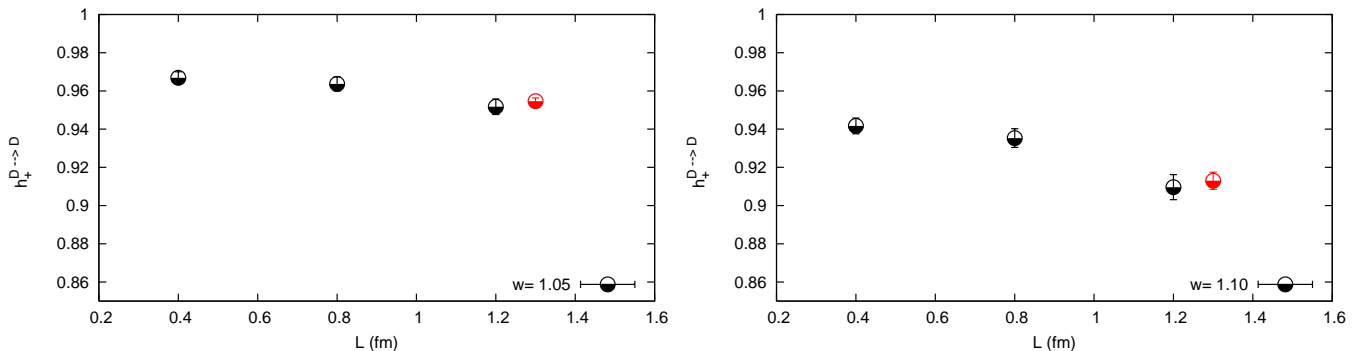


FIG. 6: $h_+^{D \rightarrow D}(w = 1.05; L)$ (left) and $h_+^{D \rightarrow D}(w = 1.10; L)$ (right) as functions of the volume. The black points have been obtained through the step scaling recursion while the red points (slightly displaced on the x -axis to help the eye) are the result of a direct simulation on the biggest volume. The data are in the continuum and chiral limits and correspond to the definition D1.

appreciable and in the case of $h_+^{i \rightarrow c}$ the σ 's are very close to one while $h_-^{i \rightarrow c}$ is affected by stronger finite volume effects. We obtain the values at $m_i = m_b$ by linear fits.

In figure 4 we plot the same quantities as in figure 3 for the second evolution step (from L_1 to L_2 , see table VI). Also in this case the step scaling functions depend very smoothly upon $1/m_i$.

C. consistency checks

In this section we illustrate the results of two checks that we have done in order to convince ourselves on the consistency of the step scaling procedure. As already discussed in sec. III, we have used two different definitions of the matrix elements and, consequently, of each form factor. In figure 5 we show the comparison of $h_+^{B \rightarrow D}(w; L)$ at $L_0 = 0.4$ fm (left) and at $L_2 = 1.2$ fm (right). We see that the results, while differing at finite volume, converge to common values after the step scaling procedure. This makes us confident of a correct accounting of finite volume effects.

A second check of the whole procedure, and in particular of the continuum limit of the step scaling functions, can be obtained by considering the elastic form factor $h_+^{D \rightarrow D}(w; L)$ at fixed w as a function of L . The point is that the charm quark mass has been simulated directly on each physical volume and, in particular, on the biggest one. In figure 6 we fix $w = 1.05$ (left) and $w = 1.10$ (right) and see that the step scaling recursion (black points) converge to the result obtained directly at $L_2 = 1.2$ fm (red points, slightly displaced to help the eye) making us confident of a correct accounting of the cutoff effects.

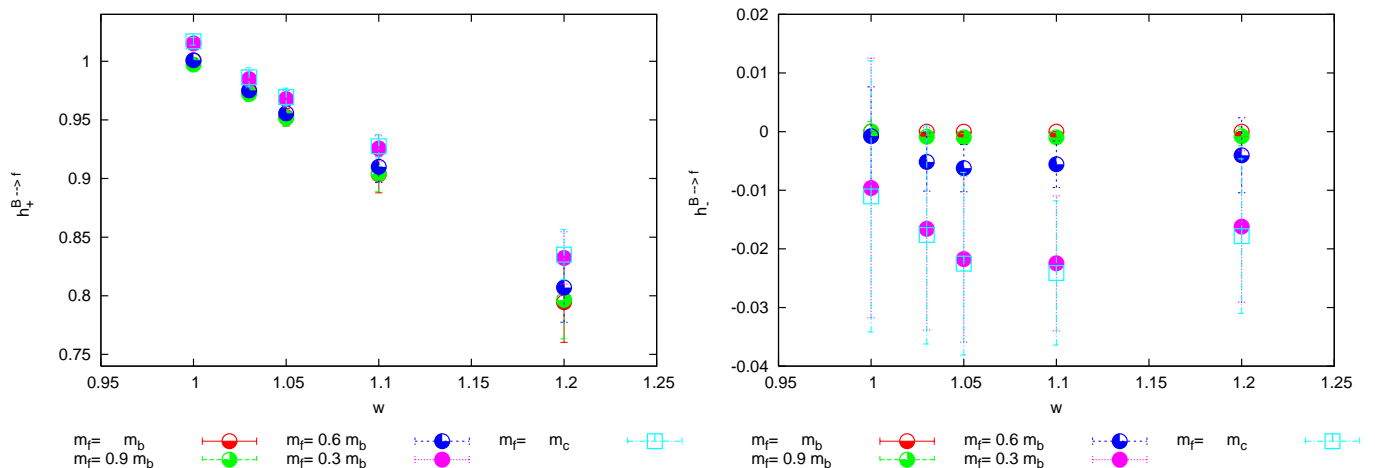


FIG. 7: In the left plot it is shown $h_+^{B \rightarrow f}(w)$ in the infinite volume limit as a function of w for different values of the final heavy quark mass. The right plot shows $h_-^{B \rightarrow f}(w)$ for the same combinations of heavy quark masses.

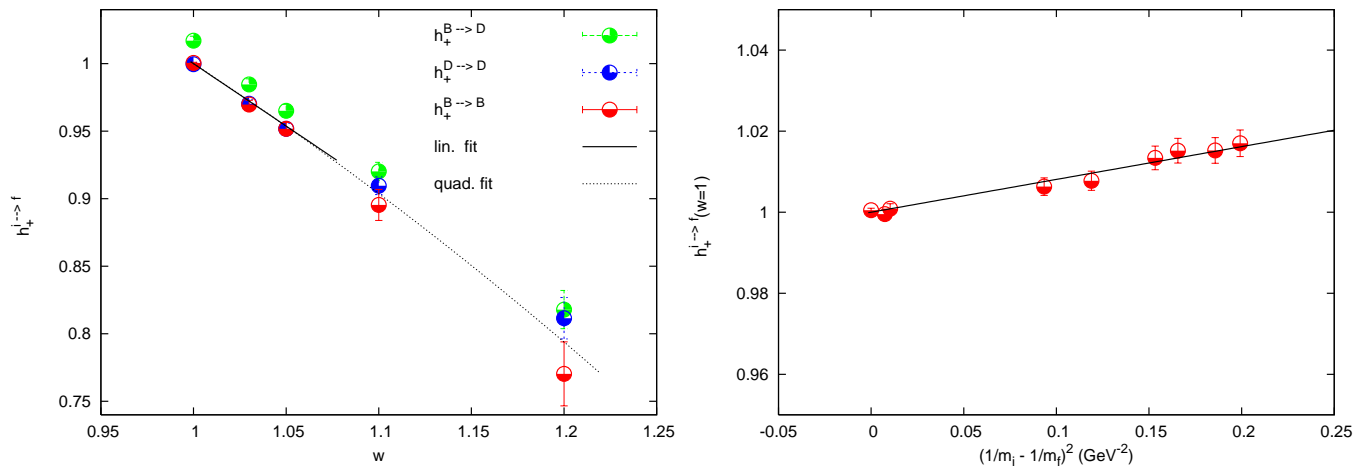


FIG. 8: The left plot shows $h_+^{B \rightarrow B}(w)$, $h_+^{B \rightarrow D}(w)$ and $h_+^{D \rightarrow D}(w)$: in the range $1 \leq w \leq 1.05$ the two elastic form factors are indistinguishable within the quoted errors while $h_+^{B \rightarrow D}(w)$ shows appreciable corrections from the Isgur-Wise limit, in particular at zero recoil. The solid line is the result of a linear fit of $h_+^{B \rightarrow B}(w)$ in the range $1 \leq w \leq 1.05$ according to eqs. (12) and (13); the dashed line is the result of a quadratic fit in the range $1 \leq w \leq 1.2$. The right plot shows $h_+^{i \rightarrow f}$ at zero recoil ($w = 1$) as a function of ε_-^2 (actually $(1/m_i - 1/m_f)^2 \propto \varepsilon_-^2$, $m_{i,f}$ being the RGI heavy quark masses): the solid line has been obtained by fitting the data according to eq. (4).

VI. FINAL RESULTS

In this section we discuss our final results in the continuum, chiral and infinite volume limits. The final values are obtained by averaging over the two definitions and by combining in quadrature statistical errors with the systematic ones due to the small residual dispersion between $D1$ and $D2$.

In order to establish the onset of the Isgur-Wise limit we plot in figure 7 the form factor $h_+^{B \rightarrow f}(w)$ as a function of w for different values of the final heavy quark mass. The right plot shows $h_-^{B \rightarrow f}(w)$ for the same combinations of heavy quark masses. We see that the corrections to the static limits of both $h_+^{B \rightarrow f}(w)$ and $h_-^{B \rightarrow f}(w)$ are of the order of 2% at the charm mass. For heavy quark masses bigger than $m_b/2$ the corrections are almost negligible (below 1%).

Eqs. (3) and (4) predict that the convergence toward the Isgur-Wise limit is faster in the case of the elastic form factors with respect to the ones having $m_i > m_f$. This happens because near the point at zero recoil the subleading corrections to $h_+^{i \rightarrow f}(w)$ are proportional to the square of the difference of the initial and final meson masses. Figure 8

$i \rightarrow f$	w	G	h_+	h_-
$D \rightarrow D$	1.00	1.000(00)	1.000(00)	
	1.03	0.971(07)	0.971(07)	
	1.05	0.955(06)	0.955(06)	
	1.10	0.916(09)	0.916(09)	
	1.20	0.828(20)	0.828(20)	
$B \rightarrow B$	1.00	1.000(00)	1.000(00)	
	1.03	0.974(07)	0.974(07)	
	1.05	0.952(07)	0.952(07)	
	1.10	0.903(16)	0.903(16)	
	1.20	0.794(34)	0.794(34)	
$B \rightarrow D$	1.00	1.026(17)	1.017(03)	-0.011(23)
	1.03	1.001(19)	0.986(08)	-0.018(19)
	1.05	0.987(15)	0.970(07)	-0.023(16)
	1.10	0.943(11)	0.928(10)	-0.024(12)
	1.20	0.853(21)	0.835(21)	-0.018(13)

TABLE I: Physical results. Average of the two definitions $D1$ and $D2$.

clearly shows that this happens in practice. Indeed, in the left plot we see that the elastic form factor $h_+^{D \rightarrow D}(w)$ is much closer to the Isgur-Wise limit (very well approximated by $h_+^{B \rightarrow B}(w)$) with respect to the form factor $h_+^{B \rightarrow D}(w)$, the one relevant into the calculation of V_{cb} . In the right plot of figure 8 we show how well eq. (4) is approximated by our numerical data. The fit is performed on the slope while the intercept is fixed to one.

For the reasons discussed above we quote as our best value for the Isgur-Wise function the results corresponding to the elastic form factor at the b -quark mass

$$\xi(w) \cong h_+^{B \rightarrow B}(w) \quad (12)$$

as given in table I. The errors quoted in this table include our estimates of the systematic errors (chiral and continuum extrapolations and residual finite volume effects).

In the literature it is usually quoted the slope of the Isgur-Wise function,

$$\xi(w) = 1 - \rho^2(w - 1) + O[(w - 1)^2] \quad (13)$$

our best result for this quantity is obtained by a linear fit of the data in the range $1 \leq w \leq 1.05$ (solid line in the left plot of figure 8)

$$\rho^2 = 0.92(15)$$

By including a quadratic term in eq. (13) and by fitting the data in the range $1 \leq w \leq 1.2$ (dashed line in the left plot of figure 8) the result changes to $\rho^2 = 0.89(17)$, i.e. much less than the quoted error. For comparison we quote the value, $\rho^2 = 0.83_{-11}^{+15+24}$, obtained by a recent quenched lattice calculation of the slope [24].

VII. CONCLUSIONS

We have performed the calculation of the form factors that parametrize semileptonic transitions among pseudoscalar heavy-light mesons. The form factors have been obtained with a relative accuracy of the order of a few percent allowing to establish the range of validity of the heavy quark effective theory for these quantities. In particular we have obtained a check of the predictions of the Luke's theorem that we re-derived. The corrections to the Isgur-Wise limit are very small already in the case of the elastic form factor $h_+^{D \rightarrow D}$ and negligible in the case of $h_+^{B \rightarrow B}$. We have also established the accuracy of the static approximation to the form factors of the decay $B \rightarrow D\ell\nu$ which is of the order of 2-3% at zero recoil and reaches about 7% at $w = 1.2$ where becomes definitely inadequate for precise phenomenological applications.

Our results have been obtained within the quenched approximation and further calculations will be needed to assess the corrections due to unquenching. On the other hand, the accuracy reached in the quenched case demonstrates the feasibility and the opportunity of repeating the present calculation in the unquenched theory. Indeed, the recursive matching process can be extended to the sea quark masses that, alternatively, can be kept to their physical values if the Schrödinger Functional formalism is used. Moreover, flavour twisted boundary conditions can be used for heavy valence quarks also in the $N_f = 3$ unquenched theory. The real case will further differ by the heavy flavour determinants that can be computed perturbatively.

Acknowledgments

We warmly thank E. Molinaro for his participation at an early stage of this work. The simulations required to carry on this project have been performed on the INFN apeNEXT machines at Rome "La Sapienza". We thank A. Lonardo, D. Rossetti and P. Vicini for technical advice.

-
- [1] N. Cabibbo, Phys. Rev. Lett. **10** (1963) 531.
 - [2] M. Kobayashi and T. Maskawa, Prog. Theor. Phys. **49** (1973) 652.
 - [3] N. Isgur and M. B. Wise, Phys. Lett. B **237** (1990) 527.
 - [4] G. M. de Divitiis, E. Molinaro, R. Petronzio and N. Tantalo, "Quenched lattice calculation of the $B \rightarrow D\ell\nu$ decay rate" [arXiv:0707.0582].
 - [5] M. Guagnelli, F. Palombi, R. Petronzio and N. Tantalo, Phys. Lett. B **546** (2002) 237 [arXiv:hep-lat/0206023].
 - [6] G. M. de Divitiis, M. Guagnelli, F. Palombi, R. Petronzio and N. Tantalo, Nucl. Phys. B **672**, 372 (2003) [arXiv:hep-lat/0307005].
 - [7] G. M. de Divitiis, M. Guagnelli, R. Petronzio, N. Tantalo and F. Palombi, Nucl. Phys. B **675**, 309 (2003) [arXiv:hep-lat/0305018].
 - [8] D. Guazzini, R. Sommer and N. Tantalo, PoS **LAT2006** (2006) 084 [arXiv:hep-lat/0609065].
 - [9] G. M. de Divitiis, R. Petronzio and N. Tantalo, Phys. Lett. B **595**, 408 (2004) [arXiv:hep-lat/0405002].
 - [10] C. T. Sachrajda and G. Villadoro, Phys. Lett. B **609**, 73 (2005) [arXiv:hep-lat/0411033].
 - [11] J. M. Flynn, A. Juttner and C. T. Sachrajda [UKQCD Collaboration], Phys. Lett. B **632**, 313 (2006) [arXiv:hep-lat/0506016].
 - [12] M. E. Luke, Phys. Lett. B **252** (1990) 447.
 - [13] A. F. Falk and M. Neubert, Phys. Rev. D **47** (1993) 2965 [arXiv:hep-ph/9209268].
 - [14] M. Luscher, R. Narayanan, P. Weisz and U. Wolff, Nucl. Phys. B **384** (1992) 168 [arXiv:hep-lat/9207009].
 - [15] S. Sint, Nucl. Phys. B **421**, 135 (1994) [arXiv:hep-lat/9312079].
 - [16] M. Guagnelli, R. Sommer and H. Wittig [ALPHA collaboration], Nucl. Phys. B **535** (1998) 389 [arXiv:hep-lat/9806005].
 - [17] S. Necco and R. Sommer, Nucl. Phys. B **622**, 328 (2002) [arXiv:hep-lat/0108008].
 - [18] M. Guagnelli, R. Petronzio and N. Tantalo, Phys. Lett. B **548**, 58 (2002) [arXiv:hep-lat/0209112].
 - [19] M. Luscher, S. Sint, R. Sommer, P. Weisz and U. Wolff, Nucl. Phys. B **491** (1997) 323 [arXiv:hep-lat/9609035].
 - [20] S. Sint and P. Weisz, Nucl. Phys. B **502**, 251 (1997) [arXiv:hep-lat/9704001].
 - [21] G. M. de Divitiis and R. Petronzio, Phys. Lett. B **419** (1998) 311 [arXiv:hep-lat/9710071].
 - [22] S. Capitani, M. Luscher, R. Sommer and H. Wittig [ALPHA Collaboration], Nucl. Phys. B **544** (1999) 669 [arXiv:hep-lat/9810063].
 - [23] M. Guagnelli, R. Petronzio, J. Rolf, S. Sint, R. Sommer and U. Wolff [ALPHA Collaboration], Nucl. Phys. B **595**, 44 (2001) [arXiv:hep-lat/0009021].
 - [24] K. C. Bowler, G. Douglas, R. D. Kenway, G. N. Lacagnina and C. M. Maynard [UKQCD Collaboration], Nucl. Phys. B **637** (2002) 293 [arXiv:hep-lat/0202029].

	β	$T \times L^3$	N_{cnfg}	k	θ
L_0A	7.300	48×24^3	277	0.124176	0.000000
				0.124844	0.953456
				0.128440	1.201080
				0.129224	2.042983
				0.131950	2.573569
				0.134041	
L_0B	7.151	40×20^3	224	0.122666	0.000000
				0.123437	0.953456
				0.127605	1.201079
				0.131511	1.719170
				0.131686	2.488490
				0.134277	
L_0C	6.963	32×16^3	403	0.120081	0.000000
				0.120988	0.953456
				0.126050	1.201079
				0.131082	1.719170
				0.131314	2.488490
				0.134526	
	0.134614				
	0.134702				

TABLE II: Table of lattice simulations of the small volume.

$i \rightarrow f$	w	G	h_+	h_-
$D \rightarrow D$	1.00	1.000(00)	1.000(00)	
	1.03	0.979(02)	0.979(02)	
	1.05	0.967(03)	0.967(03)	
	1.10	0.942(04)	0.942(04)	
	1.20	0.894(06)	0.894(06)	
$B \rightarrow B$	1.00	1.000(00)	1.000(00)	
	1.03	0.980(02)	0.980(02)	
	1.05	0.969(03)	0.969(03)	
	1.10	0.940(05)	0.940(05)	
	1.20	0.882(09)	0.882(09)	
$B \rightarrow D$	1.00	1.025(17)	1.013(03)	-0.020(37)
	1.03	1.009(14)	0.992(03)	-0.032(29)
	1.05	1.000(13)	0.980(04)	-0.040(23)
	1.10	0.976(11)	0.953(04)	-0.048(17)
	1.20	0.929(09)	0.903(06)	-0.053(12)

TABLE III: Small volume results, $L_0 = 0.4$ fm. Results corresponding to the definition $D1$.

	β	$T \times L^3$	N_{cnfg}	k	θ
L_{0a}	6.737	24×12^3	608	0.12490	0.000000
				0.12600	0.953456
				0.12770	1.201080
				0.12979	1.719172
				0.13015	2.488491
				0.13430	
				0.13460	
L_{0b}	6.420	16×8^3	800	0.120674	0.000000
				0.122220	0.953456
				0.124410	1.201079
				0.127985	1.719172
				0.128066	2.488491
				0.134304	
				0.134770	
L_{1A}	6.737	48×24^3	260	0.12490	0.000000
				0.12600	2.042983
				0.12770	2.573569
				0.12979	3.438340
				0.13015	4.976980
				0.13430	
				0.13460	
L_{1B}	6.420	32×16^3	350	0.120674	0.000000
				0.122220	2.042983
				0.124410	2.573569
				0.127985	3.438340
				0.128066	4.976980
				0.134304	
				0.134770	
	0.135221				

TABLE IV: Table of lattice simulations of the first step.

$i \rightarrow f$	w	σ_G	σ_+	σ_-
$D \rightarrow D$	1.00	1.000(00)	1.000(00)	
	1.03	0.999(01)	0.999(01)	
	1.05	0.997(02)	0.997(02)	
	1.10	0.993(03)	0.993(03)	
	1.20	0.985(05)	0.985(05)	
$B \rightarrow B$	1.00	1.000(00)	1.000(00)	
	1.03	0.997(02)	0.997(02)	
	1.05	0.996(02)	0.996(02)	
	1.10	0.991(04)	0.991(04)	
	1.20	0.981(09)	0.981(09)	
$B \rightarrow D$	1.00	1.002(02)	1.003(01)	0.89(16)
	1.03	0.999(03)	1.000(02)	0.86(13)
	1.05	0.996(04)	0.998(02)	0.83(11)
	1.10	0.991(04)	0.993(03)	0.77(08)
	1.20	0.980(05)	0.983(05)	0.72(08)

TABLE V: First step, from $L_0 = 0.4$ fm to $L_1 = 0.8$ fm. Results corresponding to the definition $D1$.

	β	$T \times L^3$	N_{cnfg}	k	θ
L_{1a}	6.420	32×16^3	360	0.126600	0.000000
				0.127400	1.603930
				0.128030	2.080840
				0.128650	2.978423
				0.129500	4.311249
				0.134304	
				0.134770	
L_{1b}	5.960	16×8^3	480	0.118128	0.000000
				0.119112	1.603930
				0.120112	2.080840
				0.121012	2.978423
				0.122513	4.311249
				0.131457	
				0.132335	
L_{2A}	6.420	48×24^3	250	0.126600	0.000000
				0.127400	2.405895
				0.128030	3.121260
				0.128650	4.467634
				0.129500	6.200000
				0.134304	
				0.134770	
L_{2B}	5.960	24×12^3	592	0.118128	0.000000
				0.119112	2.405895
				0.120112	3.121260
				0.121012	4.467634
				0.122513	6.200000
				0.131457	
				0.132335	
	0.133226				

TABLE VI: Table of lattice simulations of the second step.

$i \rightarrow f$	w	σ_G	σ_+	σ_-
$D \rightarrow D$	1.00	1.000(00)	1.000(01)	
	1.03	0.993(01)	0.993(01)	
	1.05	0.988(02)	0.988(02)	
	1.10	0.973(05)	0.973(05)	
	1.20	0.921(16)	0.921(16)	
$B \rightarrow B$	1.00	1.000(00)	1.000(00)	
	1.03	0.992(02)	0.992(02)	
	1.05	0.986(03)	0.986(03)	
	1.10	0.961(10)	0.961(10)	
	1.20	0.890(24)	0.890(24)	
$B \rightarrow D$	1.00	1.000(01)	1.000(01)	0.63(32)
	1.03	0.992(02)	0.993(02)	0.65(25)
	1.05	0.987(02)	0.988(02)	0.67(21)
	1.10	0.972(05)	0.972(05)	0.65(21)
	1.20	0.921(14)	0.921(14)	0.45(33)

TABLE VII: Second step, from $L_1 = 0.8$ fm to $L_2 = 1.2$ fm. Results corresponding to the definition $D1$.